AD 274 273

(11)

SMITHSONIAN INSTITUTION
ASTROPHYSICAL OBSERVATORY

Research in Space Science

SPECIAL REPORT
Number 84

February 9, 1962
CAMBRIDGE 38, MASSACHUSETTS

SAO Special Report No. 84

PRELIMINARY ANALYSIS OF THE ATMOSPHERIC DRAG OF THE TWELVE-FOOT BALLOON SATELLITE (1961 δ1)

by

Luigi G. Jacchia and Jack Slowey

Smithsonian Institution
Astrophysical Observatory

Cambridge 38, Massachusetts

PRELIMINARY ANALYSIS OF THE ATMOSPHERIC DRAG OF THE TWELVE-FOOT BALLOON SATELLITE (1961 δ1)[1]

by

Luigi G. Jacchia[2] and Jack Slowey[3]

(Manuscript received January 10, 1962)

Summary.--Accurate values of the atmospheric drag for the Explorer IX Satellite (1961 δ1) were computed at one-day intervals, except during magnetically perturbed days when the interval was 0.5 days. Atmospheric densities at perigee were derived by numerical integration of the drag equation, using a rotating model atmosphere with oblateness and diurnal bulge. Atmospheric temperatures were derived from Nicolet's helium-topped, diffusion-equilibrium model with asymptotically isothermal temperature profiles (Nicolet, 1961). Apart from the diurnal-bulge effect, the temperature T is well represented by $T = \text{const} + A_p + 2.5\, F_{10}$, where A_p is the daily planetary geomagnetic index and F_{10} the 10.7-cm solar flux. The temperatures derived from this satellite are in good agreement with the temperatures obtained from several other satellites during the same time interval.

---

1. Derivation of the accelerations

Secular anomalistic accelerations were derived for Satellite 1961 δ1 (Explorer IX, the 12-foot balloon satellite) using observations in the time interval February 17 to October 2, 1961. As a preliminary step, orbital elements were obtained at one-day intervals by means of the Differential Orbit Improvement (D.O.I.) Program (Veis and Moore, 1960) on the IBM 7090 calculator; these orbits will be published in separate reports by Mrs. Beatrice Miller, who was responsible for the computations.

Approximately 7100 observations were available. Of these, 2134 were field-reduced positions on photographs taken with the Smithsonian Baker-Nunn cameras; apart from a few scattered kinetheodolite measures, the bulk of the remaining observations was made by Moonwatch teams. While all observations were used for orbital computations, only the Baker-Nunn and theodolite positions were plotted to derive accelerations. The method used in deriving accelerations has been described by Jacchia (1961a). The time covered by the observations was divided into six intervals of comparable duration, taking care to have a 10-day overlap between the end of one interval and the beginning of the next. Within each interval, analytical expressions were fitted by least squares to the computed orbital elements in such a way that no appreciable systematic residuals could be detected except in the mean anomaly; in the latter, systematic residuals up to 0.001 revolutions were tolerated. The equations are given in table 1. Note that one single set of equations was used for all the elements except the mean anomaly in sections 3 and 4, and that the same was done in sections 5 and 6.

---

1. Part of this work was performed under contract with the Geophysics Research Directorate, U. S. Air Force, Cambridge; the National Aeronautics and Space Administration contributed the major support.

2. Physicist, Smithsonian Astrophysical Observatory.

3. Astronomer, Smithsonian Astrophysical Observatory.

All the satellite observations were processed a second time through the D.O.I. program -- with all the orbital elements known and defined by the equations of table 1 -- to compute individual residuals ΔM in mean anomaly for each observation. These residuals were then plotted against time and smooth curves were drawn through the plotted points. Ordinates were read off on these curves at one-day intervals, except at times of sharp inflections -- invariably connected with magnetic storms -- when the interval was reduced to 0.5 day. The table of ΔM thus obtained was then differenced to compute $d^2(\Delta M)/dt^2$. If $M_0(t)$ is the expression for M in table 1, of which ΔM are residuals, we obtain

$$\ddot{M} = \frac{d^2M}{dt^2} = \frac{d^2M_0}{dt^2} + \frac{d^2}{dt^2}\Delta M . \tag{1}$$

If the argument of perigee ω is represented by a non-linear equation, we must correct for the acceleration of the perigee, which is the origin of M. The corrected value $\ddot{M}_c$ of the acceleration in M is then

$$\ddot{M}_c = \ddot{M} + \left(\frac{dM}{dv}\right)_0 \ddot{\omega} , \tag{2}$$

where $\left(\frac{dM}{dv}\right)_0$ is the derivative of M with respect to the true anomaly v at perigee ($M = v = 0$), which is a function of the orbital eccentricity e and is given by the expansion

$$\left(\frac{dM}{dv}\right)_0 = 1 - 2e + \frac{3}{2}e^2 - \ldots . \tag{3}$$

The rate of change of the period, or secular acceleration, is clearly given by

$$\frac{dP}{dt} = \dot{P} = -\frac{\ddot{M}_c}{\dot{M}^2} . \tag{4}$$

2. Radiation pressure

Since solar radiation pressure, through periodic shadowing, contributes a large share $\dot{P}_R$ to the observed change in period for this satellite, we must correct for it if we want to obtain the atmospheric part $\dot{P}_A$ of the drag. We then have

$$\dot{P}_A = \dot{P} - \dot{P}_R . \tag{5}$$

Using the expressions of table 1 for the orbital elements, we computed $\dot{P}_R$ by means of Kozai's radiation-pressure program (Kozai, 1960); the force acting on the satellite was taken as $F_R = 4.63 \times 10^{-5} A$ (c.g.s.), where A is the presentation area of the satellite; this corresponds to a value of the solar constant of 2.00 cal cm^{-2} min^{-1}. The same program, with the same constant, accounts for the observed variation in eccentricity from February 17 to September 28, 1961, with a discrepancy of less than 1 percent, and provides a good check on the accuracy of the procedure and of the assumptions. Specifically, the eccentricity changed in that interval from 0.1223 to 0.1077. Radiation pressure accounts for a decrease in eccentricity $\Delta_1 e = -0.0128$; to this value must be added the contribution of atmospheric drag $\Delta_2 e = -0.0017$, and the contribution of the gravitational third-harmonic oscillation, which however turns out to be negligible due to the fortuitous in-phase positions of the extremes of the time interval. We are thus left with a total computed change in eccentricity $\Delta e = \Delta_1 e + \Delta_2 e = -0.0145$, against an observed value $\Delta e = -0.0146$.

3. Atmospheric densities

The rate of change of the anomalistic period P of an artificial satellite due to drag in a rotating atmosphere is very closely given (Sterne, 1958) by the equation

$$\frac{dP}{dt} = -\frac{3}{2} C_D \frac{A}{m} \rho_\pi \int_0^{2\pi} \frac{\rho}{\rho_\pi} \frac{(1 + e\cos E)^{\frac{n}{2}}}{(1 - e\cos E)^{\frac{1}{2}}} \left(1 - d\,\frac{1 - e\cos E}{1 + e\cos E}\right)^{\frac{n}{2}} dE, \qquad (6)$$

where

$$d = P\omega_s (1 - e^2)^{\frac{1}{2}} \cos i\,;$$

C_D is the drag coefficient; m the mass of the satellite; a the major axis of its orbit; ρ_π the atmospheric density at perigee height; ρ the atmospheric density at the height corresponding to a given value of the independent variable E, the eccentric anomaly; and ω_s is the angular velocity of atmospheric rotation (A and e have already been defined).

Relatively simple formulas have been derived by various authors from equation (6), with the assumption of a density scale height either constant or linear with height; more complicated formulas take into account the flattening of the atmosphere and the diurnal bulge. We have preferred to compute ρ/ρ_π directly from equation (6), using numerical integration. For the variation of ρ along the orbit, a modified version of Jacchia's atmospheric model (Jacchia, 1960) was used; the modification concerns the amplitude of the diurnal bulge which, if extrapolated beyond the height of 700 km (explicitly labelled as the upper limit), would become excessively large. Consequently, equation (10) in Jacchia's 1960 paper was changed to

$$\rho = \rho_0(z)\, F_{\xi 0}\left[1 + \varphi(z)\cos^6\frac{\psi'}{2}\right], \qquad (7)$$

with

$$\varphi(z) = 4.6 + 4\tan^{-1}[0.005(z - 600)]\,.$$

The factor $F_{\xi 0}$ is irrelevant because it is eliminated in the ratio ρ/ρ_π. With this modification the density at the center of the bulge reaches at great heights an asymptotic ratio of ten times the night-time density at the same height and is more in line with Nicolet's (1961) helium-diffusion model, which represents satisfactorily the density variations inferred from satellites with perigee above 350 km (Jacchia, 1961b). A lag angle $\lambda = 30°$ was used for the position of the bulge with respect to the sub-solar point.

The area/mass ratio of the satellite, computed from data kindly supplied by Dr. W. J. O'Sullivan of the Langley Research Center, N.A.S.A., (namely, weight 6631.5 grams, diameter exactly 12 feet) is $A/m = 15.844$ cm^2/gm. The drag coefficient C_D was taken to be 2.2; this value, which is being used in the reduction of drag data for satellites of intermediate perigee heights (300-800 km), was adopted as representing a good compromise between the extremes of 2.1 and 2.3 which can be expected for satellites of different shapes under various conditions, according to King-Hele and Walker (1961).

The derived values $\dot{P}$ and the computed values of $\dot{P}_R$ and log ρ_π are assembled in table 2.

4. Atmospheric temperatures

The perigee height of Satellite 1961 κ1 changed very rapidly because of the large effect of the radiation pressure; it rose from 640 km shortly after launching to 753 km at the end of the 7.5-month interval considered in this paper. In addition, there are periodic changes of perigee height caused by the

geometric effect of the earth's oblateness and by the third-harmonic gravitational perturbations. Under these circumstances it would be exceedingly difficult to disentangle the changes in drag due to the variable perigee height from those due to variable atmospheric structure, without the guide of an acceptable atmospheric model. Jacchia (1961b) found that the model constructed by Nicolet (1961) on the basis of diffusion equilibrium with a helium top and asymptotically-isothermal temperature profiles is n good agreement with recent results from several satellites. Since, according to Nicolet's model, the temperature is not height-dependent at the perigee heights of Sctellite 1961 ξ1, it appears useful to convert the atmospheric densities at perigee height to atmospheric temperatures and analyze the latter. This was done by a two-dimensional interpolation in Nicolet's tables, in the process of which the original data had to be very slightly smoothed.

Specifically, we proceeded as follows. Perigee heights above the geoid were computed in connection with each observed value of the drag. Six "standard" perigee heights were selected, each valid for a limited time-interval, as shown below:

	Time interval	Standard perigee height
MJD	37349 - 37393	660 km
	37394 - 37430	680 km
	37431 - 37462	700 km
	37463 - 37504	720 km
	37505 - 37574	740 km

Within each interval we reduced the atmospheric density, derived from the drag, to the "standard" perigee height using the modified Jacchia (1960) model described in section 3. Since the difference between the actual and the standard perigee height does not exceed 10 km and the scale heights are of the order of 100 km, a small inconsistency in the scale height does not appreciably affect the result.

For each of the standard heights values of log ρ were interpolated for the 12 selected temperatures used by Nicolet, and 5th-degree polynomials were fitted to the data by least squares, to express the temperature T as a function of log ρ. The temperatures derived from this satellite (see table 2) are in good agreement with the temperatures obtained from several other satellites during the same time interval.

5. Correlation of atmospheric temperatures with solar and geomagnetic data

In figure 1 the atmospheric temperatures derived from the atmospheric drag are compared with the observed values of the planetary geomagnetic index A_p and of the solar flux at 10.7 and 20 cm. Since the A_p index is a daily mean of the eight 3-hourly a_p indices, it is fair to compare it directly with the temperatures when these are computed from atmospheric drag derived with a resolution of one day. During perturbed periods (MJD 37360-37371, 37493-37501, and 37505-37510), when we used a resolution of $0^d.5$, we computed a modified "half-day A_p", by taking the mean of the four values of a_p centered around each given time.

The daily A_p's are centered around noon, G.M.T., and, roughly, so are the mean values of the 10.7-cm solar flux published by the National Research Council, Ottawa, and of the 20-cm flux published by the Heinrich-Hertz Institut, Berlin-Adlershof. For this reason, in preparing table 3, we have preferred to leave the solar and geomagnetic data in their original form and to interpolate linearly the temperatures of table 2 to show their values at 12^h G.M.T.

The correlation between the atmospheric temperatures on the one hand and the geomagnetic and solar data on the other is shown in figure 1, and is so close and evident that no additional comment is necessary. It is sufficient to say that every single geomagnetic disturbance, large or small, is reflected in a proportional temperature disturbance, and that all the fluctuations common to the curves of the 10.7-cm and 20-cm flux are present also in the temperature curve.

From a rough, preliminary analysis of the atmospheric temperatures derived from satellites when their perigee was in the dark hemisphere, Jacchia (1961b) found that the temperature increases by 3° K for each unit increase of 1 x 10^{-22} watts/m^2/cycle/second bandwidth in the 10.7-cm solar flux (F_{10}). More recent data would indicate that the coefficient dT/dF_{10} is a little lower in the vicinity of 2°.6. For the present data a coefficient of 2°.5 seems to give the best fit.

Similarly, the temperature perturbations on magnetically disturbed days are better represented for this satellite by an increase of 1°.0 per A_p unit than by the coefficient $1°.5/A_p$ as previously given by Jacchia (1962). We are referring here to moderate magnetic perturbations ($A_p < 60$); for larger perturbations the relation between such an index as A_p and the heating of the atmosphere smoothed over a finite time interval can hardly be expected to be very consistent, not to say linear. This may easily explain the difference between the two coefficients, since the value of 1°.5 was derived mostly from larger perturbations.

The last column of table 3 gives temperatures T'_π reduced to $A_p = 0$ and to $F_{10} = 100$, with the formula

$$T'_\pi = T_\pi - A_p - 2°.5\, F_{10} .$$

No values of T'_π were computed for days when A_p was greater than 30, and for the following day. It should be clear that during magnetic storms short-lived fluctuations make it impossible to apply quantitative corrections for geomagnetic activity with any accuracy comparable with that obtainable on relatively quiet days, since satellite accelerations are inevitably smoothed out by the process of double differentiation involved in their computation.

The plot T'_π at the bottom of figure 1 shows that the maxima and minima in phase with the decimetric solar flux have just about disappeared. A rising trend is visible throughout, as the perigee slowly moves toward the diurnal bulge. A quantitative analysis of the temperature variation as a function of position relative to the bulge is not justified by the small range ($< 40°$) in the angular geocentric distance ψ' between the satellite perigee and the center of the bulge. Table 4 gives, at interval of 5 days, two values of ψ', computed on the basis of a lag angle of 0° and 30° in longitude, respectively, between the bulge and the sub-solar point; the last column gives the perigee height z_π above the geoid.

Satellite 1961 δ1 is only one of nine satellites for which accurate accelerations were computed for use in a more general analysis of atmospheric properties; these preliminary results are published separately now in view of the interest that has been expressed in the performance of this particular satellite as an instrument for the determination of atmospheric densities.

References

JACCHIA, L. G.

1960. A variable atmospheric-density model from satellite accelerations. Journ. Geophys. Res., vol. 65, pp. 2775-2782.

1961a. The atmospheric drag of artificial satellites during the October 1960 and November 1960 events. Smithsonian Astrophys. Obs., Special Report No. 62, 13 pp.

1961b. A working model for the upper atmosphere. Nature, vol. 192, pp. 1147-1148.

KING-HELE, D. G. and WALKER, D. M. C.

1961. Upper-atmosphere density during the years 1957 to 1961, determined from satellite orbits. Paper presented at COSPAR Symposium, Florence, 10-14 April, 1961.

KOZAI, Y.

1960. Effects of solar radiation pressure on the motion of an artificial satellite. Smithsonian Astrophys. Obs., Special Report No. 56, pp. 25-33.

NICOLET, M.

1961. Density of the heterosphere related to temperature. Smithsonian Astrophys. Obs., Special Report No. 75, 30 pp.

STERNE T. E.

1959. Effect of the rotation of a planetary atmosphere upon the orbit of a close satellite. Journ. Amer. Rocket Soc., vol. 29, pp. 777-782.

VEIS, G. and MOORE, C. E.

1960. The Smithsonian Astrophysical Observatory differential orbit improvement program. Seminar Proceedings, Tracking Programs and Orbit Determination, Jet Propulsion Laboratory.

Table I

Least-Squares Fitting of Orbital Elements for 1961 δ1

Section 1: MJD 37347 to 37400 (February 17 - April 11, 1961)

$T_o = 37347.0$

$\omega = 101°.806 + 4°.7377\,t + °.0011\,t^2 - °.83 \times 10^{-5} t^3 - °.20 \times 10^{-7} t^4$

$\Omega = 169°.365 - 3°.6398\,t + °.89 \times 10^{-4} t^2 - °.16 \times 10^{-6} t^3$

$i = 38°.8603 + °.0011\,t - °.41 \times 10^{-4} t^2 + °.34 \times 10^{-6} t^3$

$e = .12236 - .00015\,t + .59 \times 10^{-6} t^2 + .42 \times 10^{-8} t^3$

$M = .46926 + 12.160213\,t + .51 \times 10^{-5} t^2 + .46 \times 10^{-6} t^3 - .15 \times 10^{-8} t^4$

Section 2: MJD 37390 to 37435 (April 1 - May 16, 1961)

$T_o = 37390.0$

$\omega = 306°.830 + 4°.7829\,t - °.00045\,t^2 - °.15 \times 10^{-4} t^3 + °.25 \times 10^{-6} t^4 + °.16 \times 10^{-8} t^5$

$\Omega = 13°.007 - 3°.6336\,t - °.17 \times 10^{-4} t^2 + °.50 \times 10^{-6} t^3$

$i = 38°.8557 + °.00083\,t - °.76 \times 10^{-4} t^2 + °.12 \times 10^{-5} t^3$

$e = .11729 - .97 \times 10^{-4} t + .66 \times 10^{-4} t^2 - .24 \times 10^{-6} t^3 + .25 \times 10^{-8} t^4$

$M = .39776 + 12.163319\,t + .11 \times 10^{-4} t^2 + .67 \times 10^{-6} t^3 - .74 \times 10^{-8} t^4$

Section 3: MJD 37425 to 37468 (May 6 - June 18, 1961)

$T_o = 37415.0$

$\omega = 65°.941 + 4°.7657\,t + °.22 \times 10^{-4} t^2 + °.175 \sin(166°.42 + 4°.77\,t)$

$\Omega = 282°.163 - 3°.6327\,t - °.346 \times 10^{-5} t^2 + °.36 \times 10^{-6} t^3 - °.13 \times 10^{-8} t^4$

$i = 38°.8493 - °.000565\,t + °.35 \times 10^{-4} t^2 - °.71 \times 10^{-6} t^3 + °.40 \times 10^{-8} t^4$

$e = .11617 - .85 \times 10^{-4} t + .34 \times 10^{-6} t^2 \quad .20 \times 10^{-7} t^3 + .47 \times 10^{-9} t^4 - .29 \times 10^{-11} t^5$

$M = .49293 + 12.165635\,t - .56 \times 10^{-4} t^2 + .25 \times 10^{-5} t^3 - .20 \times 10^{-7} t^4$

Table I (cont.)

Section 4: MJD 37458 to 37510 (June 8 - July 30, 1961)

$T_o = 37415.0$

$\omega = 65^\circ.941 + 4^\circ.7657\,t + {}^\circ.22 \times 10^{-4} t^2 + {}^\circ.175 \sin(166^\circ.42 + 4^\circ.77\,t)$

$\Omega = 282^\circ.163 - 3^\circ.6327\,t - {}^\circ.346 \times 10^{-5} t^2 + {}^\circ.36 \times 10^{-6} t^3 - {}^\circ.13 \times 10^{-8} t^4$

$i = 38^\circ.8493 - {}^\circ.000565\,t + {}^\circ.35 \times 10^{-4} t^2 - {}^\circ.71 \times 10^{-6} t^3 + {}^\circ.40 \times 10^{-8} t^4$

$e = .11617 - .85 \times 10^{-4} t + .34 \times 10^{-6} t^2 - .20 \times 10^{-7} t^3 + .47 \times 10^{-9} t^4 - .29 \times 10^{-11} t^5$

$M = .64170 + 12.152901\,t + .000365\,t^2 - .37 \times 10^{-5} t^3 + .14 \times 10^{-7} t^4$

Section 5: MJD 37500 to 37542 (July 20 - August 31, 1961)

$T_o = 37500.0$

$\omega = 110^\circ.991 + 4^\circ.7874\,t - {}^\circ.000148\,t^2 + {}^\circ.197 \sin(172^\circ.21 + 4^\circ.77\,t)$

$\Omega = 333^\circ.508 - 3^\circ.6268\,t - {}^\circ.94 \times 10^{-4} t^2 + {}^\circ.18 \times 10^{-5} t^3 - .11 \times 10^{-7} t^4$

$i = 38^\circ.8325 + {}^\circ.000761\,t - {}^\circ.39 \times 10^{-4} t^2 + {}^\circ.65 \times 10^{-6} t^3 - {}^\circ.41 \times 10^{-8} t^4$

$e = .11079 - .000112\,t + .44 \times 10^{-5} t^2 - .19 \times 10^{-6} t^3 + .36 \times 10^{-8} t^4 - .22 \times 10^{-10} t^5$

$M = .74612 + 12.170484\,t - .24 \times 10^{-4} t^2 + 23 \times 10^{-5} t^3 - .23 \times 10^{-7} t^4$

Section 6: MJD 37532 to 37574 (August 21 - October 2, 1961)

$T_o = 37500.0$

$\omega = 110^\circ.991 + 4^\circ.7874\,t - {}^\circ.000148\,t^2 + {}^\circ.197 \sin(172^\circ.21 + 4^\circ.77\,t)$

$\Omega = 333^\circ.508 - 3^\circ.6268\,t - {}^\circ.94 \times 10^{-4} t^2 + {}^\circ.18 \times 10^{-5} t^3 - .11 \times 10^{-7} t^4$

$i = 38^\circ.8325 + {}^\circ.000761\,t - {}^\circ.39 \times 10^{-4} t^2 + {}^\circ.65 \times 10^{-6} t^3 - {}^\circ.41 \times 10^{-8} t^4$

$e = .11079 - .000112\,t + .44 \times 10^{-5} t^2 - .19 \times 10^{-6} t^3 + .36 \times 10^{-3} t^4 - .22 \times 10^{-10} t^5$

$M = .53811 + 12.185659\,t - .000381\,t^2 + .49 \times 10^{-5} t^3 - .21 \times 10^{-7} t^4$

Table II

Satellite 1961 δ1 - Acceleration, atmospheric drag and atmospheric temperature

MJD	$-10^6 \dot{P}$	$10^6 \dot{P}_R$	$-10^6(\dot{P}-\dot{P}_R)$	$\log \rho_\pi$	T_π
37349.0	0.30	1.10	1.40	-16.533	920
50.0	0.28	1.10	1.38	.539	919
51.0	0.31	1.09	1.40	.531	922
52.0	0.34	1.08	1.42	.523	925
53.0	0.31	1.07	1.38	.532	923
54.0	0.33	1.06	1.39	.527	925
55.0	0.28	1.05	1.33	.543	921
56.0	0.31	1.03	1.34	.537	924
57.0	0.38	1.01	1.39	.518	929
58.0	0.51	0.99	1.50	.482	940
59.0	0.64	0.96	1.60	.452	949
60.0	0.49	0.94	1.43	-16.498	937
60.5	0.35	0.93	1.28	-16.546	924
61.0	0.32	0.92	1.24	.559	921
61.5	0.31	0.90	1.21	.569	919
62.0	0.29	0.89	1.18	.579	916
62.5	0.24	0.88	1.12	.601	911
63.0	0.30	0.87	1.17	.582	917
63.5	0.39	0.86	1.25	.553	925
64.0	0.64	0.85	1.49	.476	947
64.5	0.73	0.84	1.57	.454	954
65.0	0.90	0.83	1.73	.412	968
65.5	0.55	0.83	1.38	.510	939
66.0	0.26	0.82	1.08	.617	911
66.5	0.24	0.81	1.05	.630	908
67.0	0.25	0.80	1.05	.630	909
67.5	0.28	0.79	1.07	.623	912
68.0	0.31	0.78	1.09	.616	914
68.5	0.78	0.78	1.56	.461	959
69.0	0.97	0.78	1.75	.412	974
69.5	0.28	0.78	1.06	.631	913
70.0	0.23	0.78	1.01	.654	908
70.5	0.18	0.78	0.96	.677	903
71.0	0.19	0.78	0.97	-16.674	904
72.0	0.16	0.79	0.95	-16.686	903
73.0	0.23	0.80	1.03	.654	913
74.0	0.25	0.81	1.06	.645	917
75.0	0.23	0.82	1.05	.652	917
76.0	0.20	0.84	1.04	.660	917
77.0	0.25	0.85	1.10	.638	924
78.0	0.38	0.87	1.25	.586	940
79.0	0.45	0.89	1.34	.558	950
80.0	0.50	0.90	1.40	.541	956
81.0	0.51	0.92	1.43	.533	960
82.0	0.60	0.94	1.54	.501	970
83.0	0.57	0.95	1.52	.507	969

MJD	$-10^6\dot{P}$	$10^6\dot{P}_R$	$-10^6(\dot{P}-\dot{P}_R)$	$\log \rho_\pi$	T_π
37384.0	0.60	0.96	1.56	-16.496	973
85.0	0.89	0.97	1.86	.419	999
86.0	1.23	0.97	2.20	.344	1024
87.0	1.21	0.97	2.18	.346	1024
88.0	1.10	0.97	2.07	.367	1017
89.0	1.06	0.96	2.02	.375	1014
90.0	1.06	0.95	2.01	.374	1014
91.0	1.03	0.94	1.97	.380	1012
92.0	0.93	0.93	1.86	.402	1004
93.0	0.72	0.92	1.64	.454	987
94.0	0.52	0.90	1.42	.514	980
95.0	0.42	0.88	1.30	.550	968
96.0	0.44	0.87	1.31	.544	970
97.0	0.39	0.85	1.24	.566	963
98.0	0.40	0.83	1.23	.568	962
99.0	0.33	0.82	1.15	.596	954
400.0	0.31	0.80	1.11	.610	950
01.0	0.24	0.79	1.03	.642	941
02.0	0.07	0.77	0.84	.730	917
03.0	0.28	0.76	1.04	.638	943
04.0	0.79	0.75	1.54	.468	995
05.0	0.60	0.75	1.35	.526	977
06.0	0.25	0.75	1.00	.658	939
07.0	0.31	0.75	1.06	.634	947
08.0	0.21	0.75	0.96	.679	935
09.0	0.21	0.75	0.96	.681	935
10.0	0.31	0.75	1.06	.640	948
11.0	0.36	0.76	1.12	.618	956
12.0	0.41	0.76	1.17	.600	962
13.0	0.38	0.77	1.15	.609	961
14.0	0.56	0.77	1.33	.547	981
15.0	0.56	0.78	1.34	.545	983
16.0	0.60	0.78	1.44	.514	994
17.0	0.59	0.79	1.38	.532	990
18.0	0.55	0.79	1.34	.544	987
19.0	0.54	0.79	1.33	.546	987
20.0	0.44	0.78	1.22	.582	977
21.0	0.42	0.78	1.20	.587	976
22.0	0.42	0.77	1.19	.588	976
23.0	0.30	0.76	1.06	.635	962
24.0	0.29	0.74	1.03	.644	960
25.0	0.48	0.72	1.20	.574	982
26.0	0.57	0.70	1.27	.546	991
27.0	0.28	0.67	0.95	.668	953
28.0	0.09	0.64	0.73	.779	922
29.0	0.01	0.61	0.62	.847	904
30.0	0.18	0.58	0.76	.755	929
31.0	0.29	0.55	0.84	.708	953
32.0	0.41	0.52	0.93	.661	967

Table II (cont.)

MJD	$-10^6\dot{P}$	$10^6\dot{P}_R$	$-10^6(\dot{P}-\dot{P}_R)$	$\log \rho_\pi$	T_π
37433.0	0.41	0.48	0.89	-16.678	962
34.0	0.45	0.44	0.89	.676	962
35.0	0.43	0.41	0.84	.700	956
36.0	0.32	0.37	0.69	.784	932
37.0	0.41	0.32	0.73	.759	939
38.0	0.59	0.27	0.86	.688	960
39.0	0.74	0.20	0.94	.649	972
40.0	0.84	0.13	0.97	.637	977
41.0	0.96	0.08	1.04	.608	987
42.0	1.11	0.04	1.15	.575	1001
43.0	1.26	0.01	1.27	.525	1016
44.0	1.17	-0.02	1.15	.571	1002
45.0	1.10	-0.03	1.07	.606	993
46.0	1.02	-0.04	0.98	.647	981
47.0	0.91	-0.04	0.87	.703	966
48.0	0.80	-0.03	0.77	.761	950
49.0	0.86	-0.03	0.83	.733	960
50.0	0.95	-0.03	0.92	.693	974
51.0	0.97	-0.03	0.94	.689	977
52.0	0.93	-0.02	0.91	.709	972
53.0	0.87	-0.01	0.86	.739	964
54.0	0.73	0.01	0.74	.809	945
55.0	0.74	0.05	0.79	.786	953
56.0	0.84	0.13	0.97	.701	979
57.0	0.70	0.21	0.91	.733	970
58.0	0.46	0.32	0.78	.804	950
59.0	0.28	0.44	0.72	.842	939
60.0	0.14	0.56	0.70	.856	935
61.0	0.04	0.67	0.71	.851	937
62.0	-0.03	0.75	0.72	.846	938
63.0	-0.03	0.80	0.77	.817	955
64.0	-0.03	0.83	0.80	.799	961
65.0	0.03	0.85	0.88	.756	974
66.0	0.13	0.86	0.99	.702	990
67.0	0.16	0.87	1.03	.683	996
68.0	0.18	0.87	1.05	.671	999
69.0	0.30	0.87	1.17	.621	1015
70.0	0.38	0.86	1.24	.592	1025
71.0	0.70	0.84	1.54	.495	1058
72.0	0.51	0.83	1.34	.552	1038
73.0	0.49	0.82	1.31	.558	1036
74.0	0.26	0.80	1.06	.647	1006
75.0	0.12	0.79	0.91	.711	986
76.0	0.06	0.77	0.83	.748	974
77.0	-0.01	0.75	0.74	.796	960
78.0	-0.02	0.73	0.71	.813	955
79.0	-0.05	0.72	0.67	.836	949
80.0	-0.11	0.70	0.59	.891	934

Table II (cont.)

MJD	$-10^6\dot{P}$	$10^6\dot{P}_R$	$-10^6(\dot{P}-\dot{P}_R)$	$\log \rho_\pi$	T_π
37481.0	-0.14	0.69	0.55	-16.921	926
82.0	-0.14	0.68	0.54	.928	924
83.0	-0.12	0.67	0.55	.920	928
84.0	-0.08	0.66	0.58	.897	935
85.0	-0.07	0.65	0.58	.898	936
86.0	-0.03	0.64	0.61	.876	944
87.0	-0.01	0.63	0.64	.856	951
88.0	0.04	0.63	0.67	.836	958
89.0	0.02	0.62	0.64	.856	953
90.0	0.03	0.62	0.65	.850	956
91.0	0.05	0.61	0.66	.843	959
92.0	0.24	0.61	0.85	.733	994
37493.0	0.26	0.61	0.87	-16.722	998
93.5	0.47	0.61	1.08	.628	1030
94.0	0.70	0.60	1.30	.547	1058
94.5	0.77	0.60	1.37	.523	1067
95.0	1.11	0.60	1.71	.426	1104
95.5	0.97	0.59	1.56	.465	1089
96.0	0.68	0.59	1.27	.554	1057
96.5	0.55	0.59	1.14	.600	1041
97.0	0.49	0.58	1.07	.626	1032
97.5	0.51	0.58	1.09	.617	1035
98.0	0.80	0.57	1.37	.517	1071
98.5	0.99	0.57	1.56	.459	1092
99.0	1.20	0.56	1.76	.406	1113
99.5	0.79	0.55	1.34	.523	1069
500.0	0.63	0.54	1.17	.580	1048
00.5	0.59	0.54	1.13	.594	1043
01.0	0.62	0.53	1.15	.585	1046
37502.0	0.58	0.51	1.09	-16.606	1039
03.0	0.56	0.49	1.05	.619	1035
04.0	0.48	0.47	0.95	.660	1021
37505.0	0.61	0.45	1.06	-16.610	1050
05.5	0.62	0.44	1.06	.609	1050
06.0	0.28	0.42	0.70	.788	990
06.5	0.34	0.41	0.75	.757	1000
07.0	0.78	0.40	1.18	.559	1068
07.5	1.57	0.39	1.96	.337	1153
08.0	1.11	0.37	1.48	.458	1105
08.5	0.36	0.36	0.72	.771	995
09.0	0.23	0.35	0.58	.864	966
09.5	0.29	0.33	0.62	.834	975
10.0	0.24	0.32	0.56	.878	961

Table II (cont.)

MJD	$-10^6\dot{P}$	$10^6\dot{P}_R$	$-10^6(\dot{P}-\dot{P}_R)$	$\log \rho_{\pi}$	T_{π}
37511.0	0.22	0.30	0.52	-16.909	952
12.0	0.27	0.27	0.54	.892	957
13.0	0.28	0.25	0.53	.900	955
14.0	0.46	0.22	0.68	.792	989
15.0	0.51	0.20	0.71	.774	996
16.0	0.43	0.17	0.60	.849	973
17.0	0.38	0.14	0.52	.913	954
18.0	0.45	0.12	0.57	.875	966
19.0	0.57	0.08	0.65	.821	984
20.0	0.69	0.05	0.74	.767	1003
21.0	0.97	0.03	1.00	.640	1047
22.0	1.05	0.01	1.06	.619	1056
23.0	1.12	-0.01	1.11	.603	1064
24.0	0.95	-0.02	0.93	.684	1037
25.0	1.03	-0.02	1.01	.652	1049
26.0	1.10	-0.03	1.07	.632	1058
27.0	1.07	-0.02	1.05	.645	1055
28.0	1.03	-0.01	1.02	.662	1051
29.0	1.02	0.01	1.03	.661	1052
30.0	1.00	0.05	1.05	.657	1055
31.0	0.92	0.10	1.02	.673	1051
32.0	0.83	0.18	1.01	.680	1049
33.0	0.58	0.27	0.85	.756	1023
34.0	0.32	0.36	0.68	.855	992
35.0	0.22	0.44	0.66	.868	988
36.0	0.14	0.51	0.65	.874	986
37.0	0.11	0.55	0.66	.866	989
38.0	0.09	0.58	0.67	.858	991
39.0	0.09	0.60	0.69	.842	996
40.0	0.14	0.61	0.75	.803	1009
41.0	0.16	0.61	0.77	.788	1013
42.0	0.15	0.61	0.76	.790	1012
43.0	0.19	0.60	0.79	.769	1018
44.0	0.15	0.59	0.74	.793	1010
45.0	0.07	0.57	0.64	.852	990
46.0	0.11	0.55	0.66	.834	995
47.0	0.15	0.53	0.68	.818	1000
48.0	0.19	0.50	0.69	.808	1003
49.0	0.26	0.48	0.74	.774	1013
50.0	0.38	0.45	0.83	.722	1031

Table III

Atmospheric temperature compared with geomagnetic and solar data

MJD (noon)	T_π	A_p	F_{10}	F_{20}	T_π'	MJD (noon)	T_π	A_p	F_{10}	F_{20}	T_π'
37349	920	18	96	89	912	37396	966	8	98	82	963
350	920	30	99	88	892	397	962	6	104	80	946
351	924	23	100	89	901	398	958	24	96	78	944
352	924	18	102	93	901	399	952	17	93	76	953
353	924	11	103	96	905	400	946	16	92	74	950
354	923	10	104	96	903	401	929	10	89	72	947
355	922	3	106	97	904	402	930	15	88	73	945
356	926	4	101	93	920	403	969	54	93	73	-
357	934	9	103	89	917	404	986	61	98	80	-
358	949	12	103	89	929	405	958	13	103	84	-
359	943	8	103	89	927	406	943	4	105	88	927
360	929	8	103	85	913	407	941	5	107	92	918
361	918	5	104	86	903	408	936	7	105	92	917
362	916	3	96	85	923	409	942	7	103	90	927
363	931	14	94	85	932	410	952	2	104	90	940
364	958	37	93	84	-	411	959	8	103	87	943
365	940	3	95	83	-	412	962	8	105	87	942
366	910	5	94	83	-	413	971	11	111	89	932
367	912	13	90	81	-	414	982	8	111	92	946
368	944	46	91	81	-	415	988	14	126	95	909
369	941	6	98	78	-	416	997	12	120	94	935
370	906	7	92	77	919	417	988	7	114	93	946
371	904	10	93	77	912	418	987	5	121	96	930
372	908	26	91	80	904	419	982	9	122	97	918
373	916	24	98	79	897	420	976	15	124	97	901
374	918	20	99	82	900	421	976	19	119	93	909
375	917	14	98	85	908	422	969	4	110	88	940
376	920	12	101	87	906	42_	961	8	104	85	943
377	932	38	102	91	-	424	971	20	103	81	943
378	945	17	105	92	916	425	986	30	97	80	964
379	953	11	105	94	930	426	972	20	97	82	960
380	958	13	106	95	930	427	938	11	94	79	942
381	965	10	110	98	930	428	913	15	96	79	908
382	970	8	116	100	922	429	916	8	92	80	928
383	971	5	118	105	921	430	941	19	98	80	927
384	986	9	121	105	925	431	960	15	101	84	943
385	1012	22	125	108	928	432	964	22	97	83	950
386	1024	17	126	106	942	433	962	10	93	81	970
387	1020	6	126	106	949	434	959	4	91	79	977
388	1016	10	125	106	944	435	944	28	88	78	946
389	1014	6	117	102	966	436	936	8	88	78	958
390	1013	17	113	95	964	437	950	3	95	80	959
391	1008	14	105	92	982	438	966	8	100	85	958
392	996	27	101	87	967	439	974	13	105	87	949
393	984	6	103	85	970	440	982	5	110	90	952
394	974	5	107	83	951	441	990	11	109	92	957
395	969	9	106	83	945	442	1004	14	110	95	965

Insert to SAO Special Report #84

Table II (cont.)

MJD	$-10^6\dot{P}$	$10^6\dot{P}_R$	$-10^6(\dot{P}-\dot{P}_R)$	$\log \rho_\pi$	T_π
37551.0	0.51	0.43	0.94	-16.666	1050
52.0	0.57	0.40	0.97	.650	1055
53.0	0.60	0.37	0.97	.649	1056
54.0	0.71	0.35	1.06	.610	1070
55.0	0.75	0.33	1.08	.601	1073
56.0	0.78	0.31	1.09	.597	1075
57.0	0.75	0.29	1.04	.618	1068
58.0	0.74	0.27	1.01	.632	1064
59.0	0.71	0.25	0.96	.655	1056
60.0	0.69	0.24	0.93	.671	1051
61.0	0.63	0.24	0.87	.702	1041
62.0	0.55	0.23	0.78	.751	1025
63.0	0.43	0.23	0.66	.826	1001
64.0	0.35	0.23	0.58	.884	983
65.0	0.42	0.24	0.66	.831	1001
66.0	0.43	0.24	0.67	.826	1003
67.0	0.46	0.25	0.71	.804	1011
68.0	0.46	0.26	0.72	.800	1013
69.0	0.43	0.27	0.70	.814	1009
70.0	0.40	0.29	0.70	.815	1009
71.0	0.39	0.31	0.70	.816	1010
72.0	0.42	0.33	0.73	.799	1016
73.0	1.11	0.35	1.46	.498	1126
74.0	1.01	0.37	1.38	-16.523	1117

Table III (cont.)

MJD (noon)	T_{π}	A_p	F_{10}	F_{20}	T_{π}'	MJD (noon)	T_{π}	A_p	F_{10}	F_{20}	T_{π}'
37443	1009	8	108	91	981	37491	976	9	138	111	872
444	998	34	106	91	-	492	996	5	137	121	899
445	987	7	88	90	-	493	1028	102	141	116	-
446	974	6	95	88	980	494	1081	98	136	118	-
447	958	10	91	85	970	495	1080	25	136	119	-
448	955	5	91	80	972	496	1044	23	132	119	-
449	967	9	88	76	988	497	1052	36	137	131	-
450	976	22	88	76	984	498	1092	93	131	121	-
451	974	30	86	71	979	499	1080	18	126	115	-
452	968	28	88	70	970	500	1047	19	123	113	-
453	954	10	92	72	964	501	1042	35	118	110	-
454	949	8	89	73	969	502	1037	12	119	109	-
455	966	9	86	73	992	503	1028	17	118	111*	966
456	974	17	88	71	987	504	1036	13	118	112	978
457	960	24	89	72	964	505	1020	14	117	104	964
458	944	16	91	74	950	506	1029	23	115	98	968
459	937	6	100	76	931	507	1086	114	111	97	-
460	936	4	102	84	927	508	1036	18	105	90	-
461	938	2	110	85	911	509	964	8	103		948
462	947	8	108	89	919	510	957	8	92		969
463	958	3	114	90	920	511	954	6	91	71	970
464	968	4	123	97	906	512	956	8	90	76	973
465	982	11	129	100	899	513	972	42	87	76	-
466	993	10	132	102	903	514	992	18	91	79	-
467	998	6	137	106	900	515	984	18	88	77	996
468	1008	14	136	104	904	516	964	9	90	72	980
469	1020	7	131	108	935	517	960	7	92	76	973
470	1042	10	131	110	954	518	975	4	99	81	973
471	1048	58	132	113	-	519	994	17	105	86	965
472	1037	58	134	108	-	520	1025	4	113	91	989
473	1021	9	135	103	-	521	1052	11	122	97	986
474	996	6	117	100	948	522	1060	24	130	109	961
475	980	9	111	89	943	523	1050	7	128	114	973
476	967	6	108	86	941	524	1043	2	128	110*	971
477	958	7	99	76	953	525	1054	8	127	120	978
478	952	4	95	78	960	526	1056	8	123	118	990
479	942	25	102	78	912	527	1053	5	119	115	1000
480	930	4	103	77	918	528	1052	5	119	113	999
481	925	10	104	76	905	529	1054	5	116	109	1009
482	926	12	99		916	530	1053	9	113	103	1012
483	932	16	104	76	906	531	1050	6	109	102*	1022
484	936	16	103	82*	912	532	1036	5	104	96	1021
485	940	45	106		-	533	1008	2	103	90	998
486	948	16	102	88	-	534	990	3	98	87	992
487	954	14	105	94*	928	535	987	4	97	87	991
488	956	10	107	93	928	536	988	9	93	84	997
489	954	9	112		915	537	990	11	95	82	991
490	958	14	124	100	884	538	994	8	95	81*	998

Table III (cont.)

MJD (noon)	T_{π}	A_p	F_{10}	F_{20}	T_{π}'
37539	1002	5	100	83	997
540	1011	16	103	83	987
541	1012	37	106	82	-
542	1015	30	109	83	963
543	1014	28	110	84	961
544	1000	13	110	84	962
545	992	12	117	87	938
546	998	5	118	89	948
547	1002	12	114	90	955
548	1008	5	112	95	973
549	1022	4	115	99	980
550	1040	4	117	98	994
551	1052	8	126	104	979
552	1056	7	130	103*	974
553	1063	12	127	108	983
554	1072	17	130	105	980
555	1074	8	130	112	991
556	1072	28	137	113	952
557	1066	6	135	116	972
558	1060	7	133	110	971
559	1054	11	124	103	983
560	1046	7	115	96	1001
561	1033	3	108	88	1010
562	1013	9	101	83	1002
563	992	2	96	78	1000
564	992	6	92	73	1006
565	1002	2	90	75	1025
566	1007	42	97	77*	-
567	1012	35	97	82	-
568	1011	18	98	84	998
569	1009	26	96	84	993
570	1010	5	96	81	1015
571	1013	6	102	81	1002
572	1071	36	100	81	-
573	1122	114	98	78	-

Values with * are morning means, not daily means.

Table IV

Perigee height z_{π} above geoid and angular distance ψ' between perigee and diurnal bulge

MJD	z_{π} (km)	ψ' $\lambda = 0°$	ψ' $\lambda = 30°$	MJD	z_{π} (km)	ψ' $\lambda = 0°$	ψ' $\lambda = 30°$
37350	641.7	67°.4	90°.2	37465	714.0	62°.1	80°.0
355	644.1	59.9	85.7	470	712.6	52.6	73.7
360	646.6	56.1	85.0	475	712.2	44.6	69.7
365	651.2	57.4	87.2	480	714.2	40.4	67.8
370	658.0	61.4	89.7	485	718.4	39.3	66.2
375	665.8	64.4	89.9	490	723.1	38.4	63.1
380	672.3	64.0	86.9	495	726.3	35.1	58.2
385	675.7	59.8	82.0	500	727.2	29.6	53.5
390	676.2	53.9	77.9	505	727.7	25.4	52.2
395	675.4	49.2	76.4	510	727.4	28.0	56.4
400	674.8	48.1	77.5	515	728.8	37.4	64.6
405	676.6	49.9	79.2	520	732.9	48.3	73.1
410	680.8	51.6	78.8	525	738.8	56.4	78.1
415	686.1	50.5	75.0	530	744.1	59.0	77.6
420	690.3	45.6	68.6	535	746.9	55.1	71.7
425	692.4	38.5	62.7	540	746.7	45.7	63.2
430	692.6	33.9	61.0	545	744.7	33.8	55.8
435	692.7	37.2	65.6	550	742.8	25.0	53.2
440	694.9	47.6	74.6	555	742.9	26.1	55.6
445	699.8	59.5	84.0	560	745.0	34.3	60.0
450	706.0	68.7	90.3	565	747.9	41.8	62.7
455	711.4	72.4	91.0	570	750.6	44.7	61.5
460	714.0	69.7	86.8	575	753.1	41.9	56.8

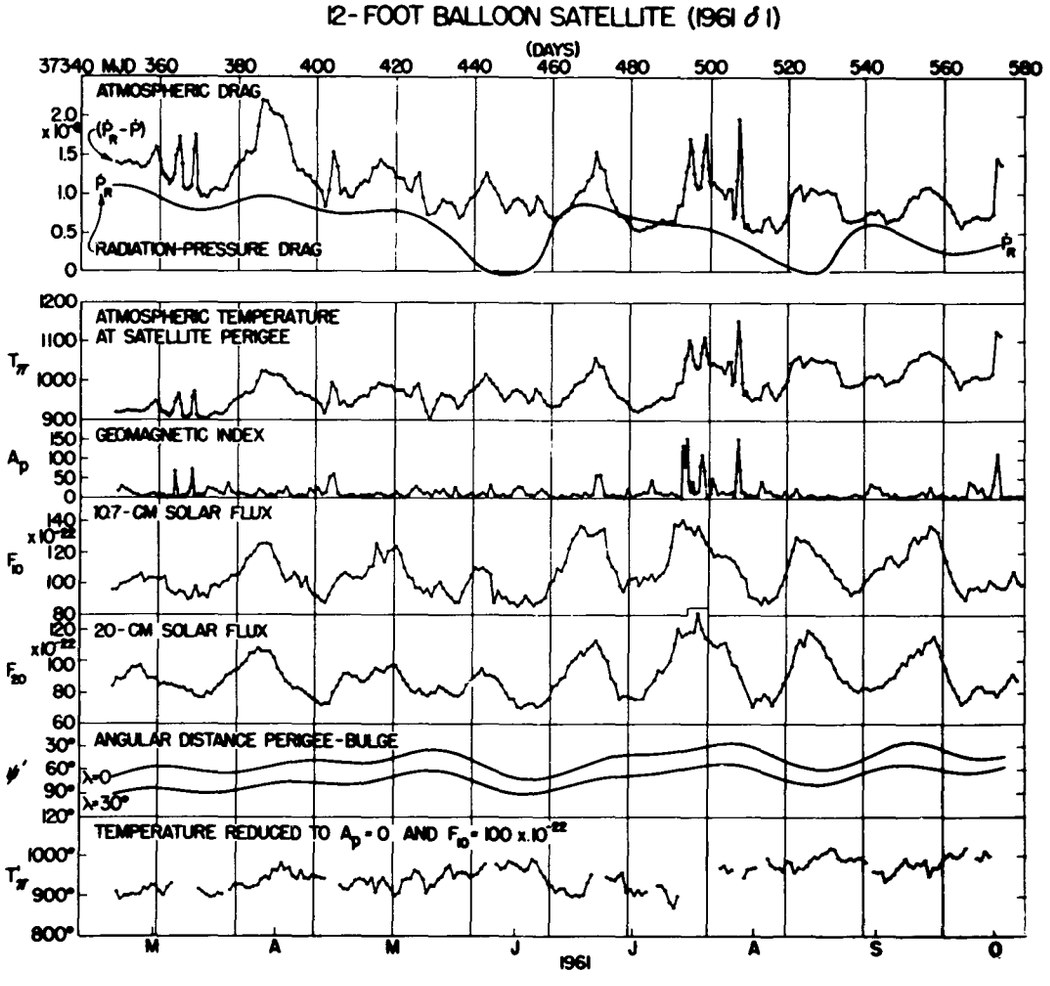

Figure 1. --Atmospheric temperatures around perigee for Satellite δ1, compared with geomagnetic activity and decimetric solar flux.

NOTICE

This series of Special Reports was instituted under the supervision of Dr. F. L. Whipple, Director of the Astrophysical Observatory of the Smithsonian Institution, shortly after the launching of the first artificial earth satellite on October 4, 1957. Contributions come from the Staff of the Observatory. First issued to ensure the immediate dissemination of data for satellite tracking, the Reports have continued to provide a rapid distribution of catalogues of satellite observations, orbital information, and preliminary results of data analyses prior to formal publication in the appropriate journals.

Edited and produced under the supervision of Mrs. L. G. Boyd and Mr. E. N. Hayes, the Reports are indexed by the Science and Technology Division of the Library of Congress, and are regularly distributed to all institutions participating in the U. S. space research program and to individual scientists who request them from the Administrative Officer, Technical Information, Smithsonian Astrophysical Observatory, Cambridge 38, Massachusetts.